THE ASTROPHYSICAL JOURNAL, 525:772–783, 1999 November 10


# STAR FORMATION IN THE ORION NEBULA CLUSTER

FRANCESCO PALLA[1] AND STEVEN W. STAHLER[2]
*Received 1999 March 3; accepted 1999 June 23*

## ABSTRACT

We study the record of star formation activity within the dense cluster associated with the Orion Nebula. The bolometric luminosity function of 900 visible members is well matched by a simplified theoretical model for cluster formation. This model assumes that stars are produced at a constant rate and distributed according to the field-star initial mass function. Our best-fit age for the system, within this framework, is $2 \times 10^6$ yr. To undertake a more detailed analysis, we present a new set of theoretical pre–main-sequence tracks. These cover all masses from 0.1 to 6.0 $M_\odot$, and start from a realistic stellar birthline. The tracks end along a zero-age main-sequence that is in excellent agreement with the empirical one. As a further aid to cluster studies, we offer an heuristic procedure for the correction of pre–main-sequence luminosities and ages to account for the effects of unresolved binary companions. The Orion Nebula stars fall neatly between our birthline and zero-age main-sequence in the H-R diagram. All those more massive than about 8 $M_\odot$ lie close to the main sequence, as also predicted by theory. After accounting for the finite sensitivity of the underlying observations, we confirm that the population between 0.4 and 6.0 $M_\odot$ roughly follows a standard initial mass function. We see no evidence for a turnover at lower masses. We next use our tracks to compile stellar ages, also between 0.4 and 6.0 $M_\odot$. Our age histogram reveals that star formation began at a low level some $10^7$ yr ago and has gradually accelerated to the present epoch. The period of most active formation is indeed confined to a few $\times 10^6$ yr, and has recently ended with gas dispersal from the Trapezium. We argue that the acceleration in stellar births, which extends over a wide range in mass, reflects the gravitational contraction of the parent cloud spawning this cluster.

*Subject headings:* open clusters and associations: individual (Orion Nebula Cluster) — stars: evolution — stars: formation — stars: pre–main-sequence

## 1. INTRODUCTION

Young stellar clusters represent promising sites for testing star formation theory. An important nearby example is the Orion Nebula Cluster, the group of low- and intermediate-mass objects surrounding the Trapezium. The four massive stars constituting the Trapezium itself have partially evacuated cloud material within a volume several pc in radius, allowing optical study of this extensive population. Herbig & Terndrup (1986) identified 150 stars over an area of $3' \times 3'$, and estimated the stellar density to be in excess of $2 \times 10^3$ pc$^{-3}$. More recent optical and near-infrared studies have surveyed out to some 2.5 pc from the Trapezium, revealing several thousand additional stars (McCaughrean & Stauffer 1994; Prosser et al. 1994; Ali & Depoy 1995; Hillenbrand 1997). With its peak density now estimated at $2 \times 10^4$ pc$^{-3}$, the Orion Nebula Cluster is easily the most crowded aggregate of young stars in the solar neighborhood.

There are two known methods for quantitatively gauging the star formation activity within any region. The first is to make an accurate compilation of the luminosity function. Comparison of this function with a theoretical model then yields both the system's composite age and the evolutionary status of member stars, although the latter is only obtained in a statistical sense (Zinnecker, McCaughrean, & Wilking 1993; Fletcher & Stahler 1994a, 1994b; Lada & Lada 1995). The second, and more precise, technique is to place the stars in the H-R diagram. One can then read off directly the ages and masses of individual cluster members. The result is a detailed history of stellar births, as well as the relative production rates of various masses.

In the case of Orion, the study by Hillenbrand (1997) has provided an especially rich trove of empirical data. Hillenbrand was able to measure the $V$- and $I$-band luminosities for over 900 stars within 2.5 pc of the Trapezium. Applying a bolometric correction to the $I$-magnitudes, she obtained values of $L_*$ for this large sample. She then used the $V-I$ colors to ascertain $T_{\rm eff}$, after correcting for interstellar extinction. Her placement of the cluster members in the H-R diagram confirmed the extreme youth of the region, with the mean stellar age falling under $1 \times 10^6$ yr. She also found a mass spectrum heavily weighted toward low-mass stars. The actual distribution was roughly a power law above 0.2 $M_\odot$. One curious result was that the cluster members of intermediate mass appeared to be systematically older, on average, than their low-mass counterparts.

The general conclusions of this and previous studies are consistent and seem firmly established. Quantitative findings, however, are sensitive to the particular choice of theoretical pre–main-sequence evolutionary tracks. Both Hillenbrand (1997) and other investigations have relied on the tracks produced by D'Antona & Mazzitelli (1994) and Swenson et al. (1994). In addition to giving disparate results, both of these calculations utilized essentially arbitrary initial conditions for pre–main-sequence contraction. One should more properly begin each star with the properties inherited from its prior epoch of protostellar accretion. The corrected tracks then start from a rather well defined birthline in the H-R diagram (Stahler 1983, 1988). Correction of pre–main-sequence ages is substantial for intermediate-

[1] Osservatorio Astrofisico di Arcetri, Largo E. Fermi 5, 50125 Florence, Italy; palla@arcetri.astro.it.
[2] Berkeley Astronomy Department, University of California, Berkeley, CA 94720; Sstahler@astro.berkeley.edu.

mass objects (Palla & Stahler 1990), and for *all* stars in a system younger than a few million yr.

Our purpose, then, is to reassess star formation activity within the Orion Nebula Cluster. We first present, in § 2, an improved set of evolutionary tracks, covering all masses of relevance. These results will naturally be of interest for many studies beyond the present one. Section 3 then utilizes the statistical model of Fletcher & Stahler (1994a) to analyze the region's bolometric luminosity function. Here we find that the data bolster the underlying model assumptions, and we estimate a new age of $2 \times 10^6$ yr for the cluster as a whole. Our more detailed study of formation activity is presented in § 4, where we derive masses and ages from the H-R diagram. We confirm that stars have been produced in rough accordance with the field-star initial mass function, but see no correlation between mass and age. On the contrary, our most significant finding is a dramatic acceleration of star formation that occurs over a broad mass range. We finally argue in § 5 that this trend signifies a global contraction of the parent molecular cloud. The appearance of the Trapezium itself must have been a relatively late event in the contraction process.

## 2. NEW PRE–MAIN-SEQUENCE TRACKS

According to the classical theory initiated by Hayashi (1961), a star of any mass begins its pre–main-sequence lifetime with a radius well in excess of the corresponding main-sequence value. The large surface area implies a high luminosity, more than can be transported by radiation alone. Thus, all pre–main-sequence stars were thought to begin as fully convective objects. In the H-R diagram, their evolutionary tracks spanned a broad area above the zero-age main sequence (ZAMS). Other researchers later added quantitative details, especially regarding the ignition of light elements and the final approach to the main sequence (Iben 1965; Bodenheimer 1966; Ezer & Cameron 1965). Calculations of this type have more recently been continued by D'Antona & Mazzitelli (1994), Swenson et al. (1994), and others (e.g., Forestini 1994; Chabrier & Baraffe 1997).

Prior to their quasi-static contraction, stars are embedded objects still gathering mass from their parent interstellar clouds. Detailed studies of the protostar phase led, by the early 1980s, to a significant alteration of pre–main-sequence theory. In particular, it was recognized that the starting radius for a star must be that attained during its protostellar accretion phase. This requirement is equivalent to the condition that pre–main-sequence tracks begin from a certain curve, or birthline, in the H-R diagram (Stahler 1983). Earlier researchers had noted, in fact, that T Tauri stars rarely appear higher than the so-called "deuterium main sequence" (Larson 1972; Grossman & Graboske 1973). Within the classical theory, this was the locus in the diagram where the stars' central temperatures reached about $10^6$ K, so that the residual supply of interstellar deuterium could fuse with protons to form $^3$He (see, e.g., Clayton 1983). It was at first puzzling that this event should have any bearing on observed pre–main-sequence stars, especially after Stahler, Shu, & Taam (1980) pointed out that deuterium is likely to be exhausted in the earlier, protostar phase. However, Stahler (1988) showed that the protostar's radius during accretion, and therefore the actual position of the birthline, is largely set by the thermostatic effect of the fusion process. Thus, the birthline at lower masses coincides approximately with the old deuterium main sequence, and also forms the upper envelope to the distribution of T Tauri stars.

The situation changes for objects of intermediate mass, i.e., those exceeding about 2 $M_\odot$. Here, the stellar luminosity is high enough that deuterium fusion is energetically minor during the accretion phase. The predicted radii at the onset of pre–main-sequence evolution are no longer much greater than those on the main sequence. Indeed, Palla & Stahler (1990) demonstrated that the two radii coincide, i.e., that the birthline intersects the ZAMS, at a relatively modest mass value. Stars of somewhat lower mass begin as radiatively stable objects and undergo an upward shift in luminosity before joining onto the horizontal portions of their classical tracks (Stahler 1989). Since the deuterium thermostat is no longer operative, the position of the birthline is more sensitive to such factors as the protostellar mass accretion rate, $\dot{M}$. Palla & Stahler (1990) found that the theoretical curve matches the upper envelope of Herbig Ae and Be stars for an assumed rate of $\dot{M} = 1 \times 10^{-5}\ M_\odot\ \mathrm{yr}^{-1}$. Here the birthline terminates at 8 $M_\odot$. More generally, the calculated reduction in pre–main-sequence lifetime (relative to the classical, Kelvin-Helmholtz value) is more severe than for the low-mass T Tauri stars.

In principle, the accretion rate should not be assigned a priori but obtained from a separate calculation of cloud dynamics. Such collapse studies continue to indicate that an $\dot{M}$-value near $10^{-5}\ M_\odot\ \mathrm{yr}^{-1}$ is reasonable (Masunaga, Miyama, & Inutsuka 1998). On the other hand, the detailed temporal behavior of the function varies with initial and boundary conditions (Foster & Chevalier 1993). These factors in turn depend on the physical state of the cloud fragment (dense core) *prior* to collapse. Of particular significance is the manner in which the ambient magnetic field relinquishes mechanical support (Basu & Mouschovias 1995; Safier, McKee, & Stahler 1997; Li 1998). While awaiting further developments on such issues, it is still important to have a complete and numerically detailed set of pre–main-sequence tracks, utilizing a plausible set of initial conditions supplied by protostar theory.

This task was begun by Palla & Stahler (1993), who obtained tracks for stars with masses from 1.0 to 6.0 $M_\odot$. In each case, the initial model was taken from the sequence of protostars calculated by Palla & Stahler (1992), again for $\dot{M} = 1 \times 10^{-5}\ M_\odot\ \mathrm{yr}^{-1}$. Neglecting internal rotation, magnetic fields, and the effect of winds, we assumed the star to be a sphere of constant mass as it contracted from the birthline to the ZAMS. The only element apart from hydrogen whose fusion we followed was deuterium, whose initial abundance was taken from the protostar models. Note that protostars with $M_* \gtrsim 1\ M_\odot$ contain deuterium only in a thin surface layer, so that it is rapidly destroyed during subsequent contraction. The fusion of ordinary hydrogen was followed through both the *pp* chains and the CN cycle.

We have now extended this work into the regime of low-mass stars. The initial protostellar models are taken from Stahler (1988), who covered the range from 0.1 to 1.0 $M_\odot$. Here we again selected the model sequence corresponding to $\dot{M} = 1 \times 10^{-5}\ M_\odot\ \mathrm{yr}^{-1}$. Starting from these states, we have obtained pre–main-sequence tracks for 0.1, 0.2, 0.4, 0.6, and 0.8 $M_\odot$. The numerical procedure is identical to that in Palla & Stahler (1993), as are the physical approximations. In particular, we continue to neglect both the thermal effect of stellar winds and their associated mass loss. Empirical determination of the mass outflow in

T Tauri stars remains problematic, with most estimates utilizing the high-velocity component of the optical forbidden line emission occurring within 100 AU of the star (e.g., Edwards, Ray, & Mundt 1993). The studies of Hartigan, Edwards, & Ghandour (1995) and Hirth, Mundt, & Solf (1997) obtain rates on the order of $10^{-9}\ M_\odot\ \mathrm{yr}^{-1}$ for a sample of about 40 T Tauri stars. Since the typical age of these stars is a few $\times\ 10^6$ yr, their reduction of mass has been relatively small; so is any *increase* of mass, which presumably occurs through circumstellar disk accretion. Recently, Gullbring et al. (1998) and Hartmann et al. (1998) analyzed ultraviolet, optical, and infrared lines in a sample of 60 stars in the Taurus and Chamaeleon I cloud complexes. They find typical disk accretion rates of $10^{-8}\ M_\odot\ \mathrm{yr}^{-1}$, again too small for significant mass change during the earliest, active phase.

One departure from our earlier work concerns the stellar opacity. In the lower temperature regime, we now utilize the Rosseland mean opacities of Alexander & Ferguson (1994). Above $10^4$ K, we have employed the OPAL compilation of Iglesias & Rogers (1996) for a gas of Population I composition ($X = 0.70$, $Y = 0.28$). The two calculations agree to within a few percent for temperatures between $8 \times 10^3$ and $1 \times 10^4$ K. Note that the opacities of Iglesias & Rogers are higher than our previous values by as much as a factor of 3 at a temperature of a few $\times\ 10^4$ K. This change, which stems from improved treatment of partially ionized iron, has had a major impact on stellar pulsation models (Iglesias & Rogers 1991). However, its effect is rather modest on evolutionary tracks in the H-R diagram.

More significant in this regard is the opacity at lower temperatures. Here the effect of molecules predominates, and it remains difficult to gauge accurately. For a star of subsolar mass that is largely or fully convective, the computed radius and effective temperature are sensitive to the subphotospheric conditions (see the discussion in Allard et al. 1997). As an illustration, we have compared pre–main-sequence tracks for masses between 0.6 and 1.0 $M_\odot$ using the Alexander, Johnson, & Rypma (1983) opacities and those of Alexander & Ferguson (1994). Note that the revised values depart significantly from the older set only for $T_{\rm eff} \lesssim 4 \times 10^3$ K. We find that the current models of lowest mass have smaller effective temperatures (at the same age), by as much as 150 K. Recently, Alexander et al. (1998) have extended their calculations below 2000 K, where a variety of grains condense. Our coolest models have effective temperatures near 3000 K, and we therefore neglected the grain contribution. However, we emphasize that stars less massive than about 0.4 $M_\odot$ would more accurately be treated by attaching a detailed stellar atmosphere model to the interior calculation. Pending such an improvement, the reader should view our results in this regime with due caution.

Another complication at lower masses is the equation of state, for which the recombination of molecular hydrogen, Coulomb interaction, and pressure ionization all become significant. We have continued to rely on the tabulation of Eggleton, Faulkner, & Flannery (1973), but have supplemented this with the more recent results of Pols et al. (1995). These latter authors have treated pressure ionization in an approximate, analytic fashion, but obtain good agreement with the more detailed calculations of Mihalas, Däpper, & Hummer (1988) and Rogers, Swenson, & Iglesias (1996). Nevertheless, our prescription for both the opacity and the equation of state precludes us from extending our calculation into the brown dwarf regime, where a more careful treatment is essential (see, e.g., Saumon, Chabrier, & Van Horn 1995).

As in our earlier study, we have only tracked deuterium among the light elements consumed before ordinary hydrogen. The next most abundant species, lithium, has too small a fractional abundance to be significant energetically. (See Ventura et al. 1998 for a recent discussion of lithium depletion in pre–main-sequence models.) We took the initial deuterium abundance at each mass from the protostar sequence of Stahler (1988). For our adopted mass accretion rate, burning starts at a protostellar mass of 0.3 $M_\odot$, and the abundance drops to less than 0.1 times the full interstellar value by 0.9 $M_\odot$. For the latter, we assumed a number fraction relative to hydrogen of $[\mathrm{D/H}] = 2.5 \times 10^{-5}$, which is at the high end of currently accepted values (Linsky 1998; Geiss & Glockner 1998; Vidal-Majar, Ferlet, & Lemoine 1998). In summary, most of our pre–main-sequence models begin their contraction with a significant depletion of deuterium.

The remaining input physics is identical to our previous study. We treat convection according to standard mixing-length theory, employing a ratio of mixing length to local pressure scale height of 1.5. Figure 1 displays our full set of tracks in the H-R diagram, together with the birthline and selected isochrones.[3] Note the smooth transition at the joining masses of 1.0 and 0.8 $M_\odot$. One test of the tracks' quantitative reliability is through comparison of our theoretically derived ZAMS and the diagrams of young, open clusters. In this regard, we find that the observed lower envelope of the Pleiades shows no significant departure

[3] The complete set of tracks and isochrones is available upon request from the author.

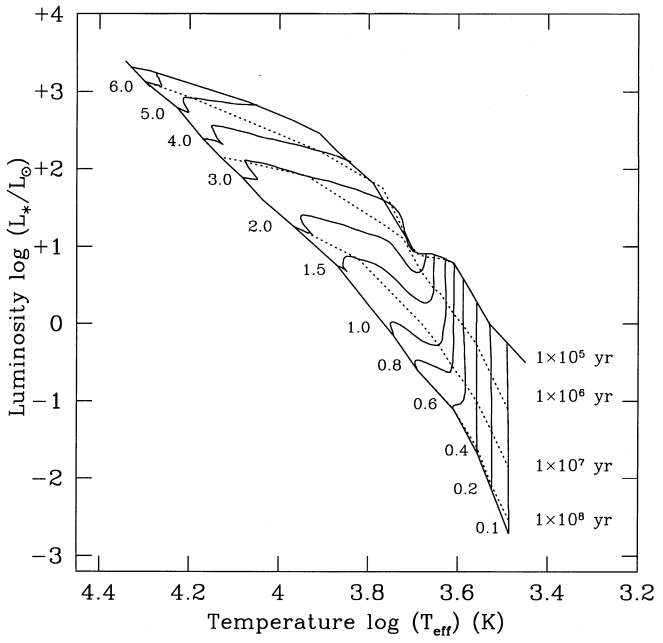


FIG. 1.—Theoretical pre–main-sequence tracks in the H-R diagram. Each track is labeled by the corresponding stellar mass, in units of $M_\odot$. Selected isochrones are shown by the dotted lines. For each track, the evolution starts at the birthline (*light solid line*), and ends at the ZAMS, also indicated.

TABLE 1

CHARACTERISTIC TIMES OF PRE–MAIN-SEQUENCE EVOLUTION

| Mass ($M_\odot$) | $\Delta t_D$ (yr) | $t_{rad}$ (yr) | $t_{ZAMS}$ (yr) |
|---|---|---|---|
| 0.1..... | $1.5 \times 10^6$ | ... | $3.7 \times 10^8$ |
| 0.2..... | $7.0 \times 10^5$ | ... | $2.4 \times 10^8$ |
| 0.4..... | $3.0 \times 10^5$ | $1.1 \times 10^7$ | $1.1 \times 10^8$ |
| 0.6..... | $2.0 \times 10^5$ | $5.5 \times 10^6$ | $8.5 \times 10^7$ |
| 0.8..... | $1.5 \times 10^4$ | $2.5 \times 10^6$ | $5.2 \times 10^7$ |
| 1.0..... | ... | $1.4 \times 10^6$ | $3.2 \times 10^7$ |
| 2.0..... | ... | ... | $8.5 \times 10^6$ |
| 3.0..... | ... | ... | $2.0 \times 10^6$ |
| 4.0..... | ... | ... | $8.2 \times 10^5$ |
| 5.0..... | ... | ... | $2.3 \times 10^5$ |
| 6.0..... | ... | ... | $4.0 \times 10^4$ |

from our curve, at least down to 0.1 $M_\odot$ (see, e.g. Meynet, Mermilliod, & Maeder 1993). Here we have assumed the traditional cluster distance of 130 pc, which is consistent with the recent *Hipparcos* data (Pinsonneault et al. 1998). Below 0.6 $M_\odot$, our ZAMS passes close to the location of the eclipsing binaries YY Gem and CM Dra (Viti et al. 1997; Bessell 1998), and to the M dwarfs observed by Kirkpatrick et al. (1993) and Leggett et al. (1996).

We list other key features of our tracks in Table 1. For each low-mass star, the second column gives $\Delta t_D$, the duration of deuterium burning. This interval is measured to the point at which [D/H] falls to 0.1 of its value on the birthline, but only for those masses for which the *initial* abundance is at least 0.1 of interstellar. We next list $t_{rad}$, the time at which a radiatively stable core first appears in fully convective models. Here $t = 0$ refers to the star's appearance on the birthline. Finally, the fourth column gives $t_{ZAMS}$, the total time required for each star to settle onto the ZAMS. We rather arbitrarily set the latter at the point where the luminosity released through gravitational contraction falls to 3% of the total.

Comparison of our results with those of other authors reveals significant differences, reflecting the influence of both starting conditions and input physics. The widely used calculation of D'Antona & Mazzitelli (1994) treated convection according to the turbulence model of Canuto & Mazzitelli (1991). Their tracks exhibit much greater curvature than either our models or older ones, even in the fully convective phase. The D'Antona & Mazzitelli models also have higher surface temperatures at the earliest ages. For masses between 0.4 and 1.5 $M_\odot$, our $T_{eff}$ values are lower by about 400 K. Conversely, a young pre–main-sequence star that we gauge to have 0.4 $M_\odot$ would have only 0.2 $M_\odot$ according to their calculation. Equally severe are the discrepancies in age. The birthline reduces our ages for intermediate masses, as explained above. At the lowest masses, the D'Antona & Mazzitelli isochrones sag below ours, and even below the empirical ZAMS. Thus, a star of a given $L_*$ and $T_{eff}$ has a lower age than we would obtain. All these differences, needless to say, have a profound impact on the interpretation of cluster diagrams.[4]

[4] Recently, D'Antona & Mazzitelli (1998) have presented results with an altered convection model. While the main differences with our tracks remain, their $T_{eff}$ values for low masses are now reduced by about 100 K, and their theoretical ZAMS is in closer accord with the empirical one.

## 3. LUMINOSITY FUNCTION

One of the most important uses of pre–main-sequence tracks is to assess the evolutionary status of young clusters. For those that are too embedded to measure reliable effective temperatures, the observed luminosities are still of value in this regard. Much of the Orion Nebula Cluster *is* optically revealed, because of clearing by the central Trapezium stars. It is nevertheless instructive to use the existing compilation of luminosities as a diagnostic tool, both to illustrate the method and to compare its results with those obtained through other techniques.

Pre–main-sequence theory gives the evolution of the bolometric luminosity, $L_*$, for a given stellar mass. To go further and predict the spectral energy distribution, one must first know the effective temperature, which theory also provides. Unfortunately, young stars with ages of a few $\times 10^6$ yr or less commonly have excess emission at infrared wavelengths (for the specific case of Orion, see McCaughrean & Stauffer 1994; Hillenbrand et al. 1998). It has long been accepted that this emission stems from the heating of nearby dust, much of it contained in residual circumstellar disks. This material gradually spirals onto the star through internal torquing. Our understanding of the process is still inadequate for quantitative predictions. The emphasis, rather, has been on using observed spectral energy distributions to infer disk properties (see, e.g., Beckwith et al. 1990). These studies have shown, for example, that a significant gap may exist between the stellar surface and the inner disk edge (Calvet et al. 1991).

Surveys of the most obscured clusters, such as $\rho$ Ophiuchi or IC 348, are still limited, in the main, to near-infrared wavelengths. Motivated by this practical consideration, various researchers have developed theoretical models of the $K$-band luminosity function and applied these to actual systems (Zinnecker et al. 1993; Lada & Lada 1995). These authors circumvented the infrared-excess problem by assuming a main-sequence spectral energy distribution in their model stars. Zinnecker et al. (1993) further assumed that all members within a cluster begin their quasi-static contraction at the same instant of time. Utilizing traditional pre–main-sequence tracks, they found a sharp peak in their $K$-band luminosity functions, which they associated with the deuterium main sequence (see also the discussion in Prusti 1999). However, Lada & Lada (1995) found better agreement with observations by spreading out in time the onset of contraction.

Fletcher & Stahler (1994a; 1994b) developed a more detailed statistical model, utilizing only the bolometric luminosity function and accounting for modern developments in pre–main-sequence theory. In their hypothetical cluster, the first dense core begins collapsing dynamically at some definite but arbitrary time, $t = 0$. Other cores follow suit, at an assumed global rate designated $C(t)$. Every collapse builds up a central protostar at the rate $\dot{M}$; here this quantity is taken to be a temporal constant. Each protostar, moreover, has a certain probability per unit time for dispelling its cloud envelope and appearing on the birthline as a pre–main-sequence object. This probability is determined by requiring that all cluster members ultimately be distributed according to a standard field-star initial mass function. One can then add together the protostellar (accretion) and pre–main-sequence luminosities at each epoch to obtain the total luminosity function.

In practice, the model requires both a value for the protostellar mass accretion rate and specification of the global collapse rate $C(t)$. The former, as we have indicated, follows in principle from studies of cloud collapse. There is as yet no equivalent theoretical basis for $C(t)$. For simplicity, Fletcher & Stahler took this rate to be a strict constant. The actual value of the luminosity function for any $L_*$ is directly proportional to $C(t)$ (see, e.g., eq. [37] of Fletcher & Stahler 1994a). A temporally constant value therefore behaves as a simple scale factor, and does not affect the intrinsic form of the luminosity function. In the end, the model function depends only on $\dot{M}$ and the evolutionary time $t$. One can thus compare a sequence of predicted functions with observations to read off the best value of $t$. Fletcher & Stahler (1994b) followed this procedure for the L1688 cluster in $\rho$ Ophiuchi, utilizing the subsample of bolometric luminosities previously obtained through spectral integration by Wilking, Lada, & Young (1989). The best-fit age of $t = 1 \times 10^6$ yr agreed with the limited data available from optically visible members (see also Bouvier & Appenzeller 1992).

Returning to Orion, the histogram in Figure 2 shows the empirical bolometric luminosity function, $\Phi_*(L_*)$, for 940 stars, taken from the study of Hillenbrand (1997). Here $\Phi_*$ is defined as the number of stars per logarithmic unit of luminosity. The individual values of $L_*$ were obtained not by direct integration as in the much smaller $\rho$ Ophiuchi sample, but through the application of a main-sequence bolometric correction to the dereddened $I$-band fluxes. Hillenbrand tested the accuracy of this method by using it to calculate $L_*$ for a previously studied sample in Taurus. Here she found good agreement with the $L_*$ values obtained using either high-resolution optical spectra (Hartigan et al. 1995) or extinction-corrected $J$ magnitudes (Kenyon & Hartmann 1995).

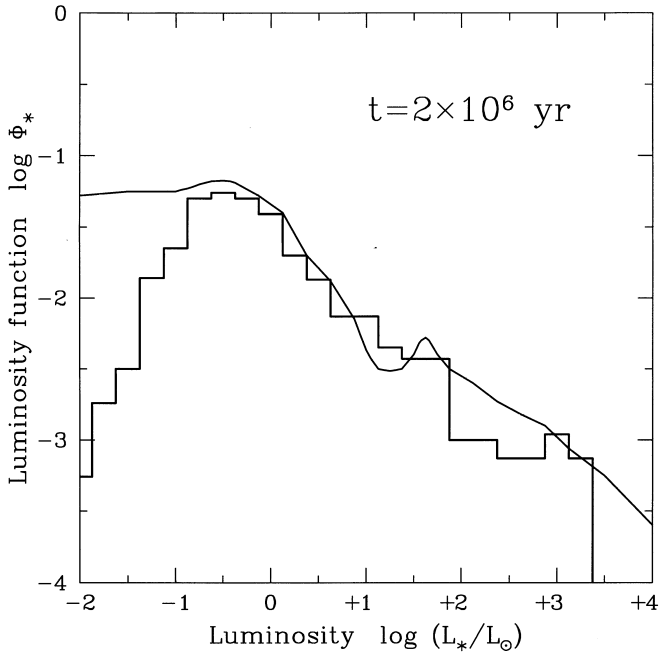


FIG. 2.—Bolometric luminosity function of the Orion Nebula Cluster. The lighter histogram shows the empirical distribution for 940 stars, taken from Hillenbrand (1997). The heavy solid curve shows the theoretical prediction for the indicated age.

The smooth curve in the figure represents the best-fit theoretical luminosity function. Following Fletcher & Stahler (1994a), the actual pre–main-sequence tracks used in calculating $\Phi_*(L_*)$ are not those depicted in Figure 1, but an earlier compilation from various authors. These published tracks were truncated at the upper end by using the protostellar mass-radius relation from Stahler (1988) and Palla & Stahler (1991). After appropriately resetting the individual contraction times, both the tracks and isochrones are quite similar to those presented in § 2. The resulting luminosity function thus differs little from one derived using the later tracks.[5]

It is evident that the theoretical curve reproduces the general rise in $\Phi_*$ toward lower luminosities. This agreement bolsters the model assumptions, including a stellar mass distribution that follows the field-star function. On the other hand, the empirical histogram falls well below our curve for the lowest values of $L_*$. A similar departure occurs in $\rho$ Ophiuchi, but starting at much higher luminosity (see Fig. 17 of Fletcher & Stahler 1994b). In both cases, the empirical decline is due to the limited sensitivity of the survey in question. Hillenbrand (1997) claims 90% completeness of her observations down to an apparent $I$-band magnitude of 17. At the distance of Orion, the latter figure corresponds to $L_* = 0.1\ L_\odot$, assuming a typical extinction of $A_V = 2$ mag. This luminosity bound is in good accordance with the falloff seen in Figure 2.

The underlying statistical model assumes a constant star formation rate $C(t)$, so the derived age of $2 \times 10^6$ yr must represent some kind of average value. We clarify this notion in the next section, after we utilize the additional information available from stellar spectra. In any case, the estimated time is accurate to within about 50%. Thus, the theoretical curve for $t = 1 \times 10^6$ yr is too high at low luminosities, and dips below the data for $\log L_* \lesssim 0$. Note finally the small hump in the curve near $\log L_* = +2$. This feature represents the contribution to the total luminosity function from accreting protostars. Since the latter are deeply embedded objects, the hump should more properly be deleted for the present comparison. The resulting theoretical curve, representing main-sequence and pre–main-sequence stars only, would not change significantly.

## 4. STELLAR MASSES AND AGES

Having obtained a preliminary view of the cluster's history, we now utilize the compilation of effective temperatures. Figure 3 displays the H-R diagram for 705 stars. This subsample represents those optically visible objects from Hillenbrand (1997) that have an estimated membership probability exceeding 67%. Here the probability is based on various proper-motion studies.[6] For 163 of the remaining 235 stars, no membership information is available from the literature. In fact, the luminosities and effective temperatures within this latter group are generally consistent with our selected objects, so that the majority are undoubtedly members as well. Our rather conservative selection criterion still leaves us with a sample large enough to draw statistically meaningful conclusions. Note finally that this population includes all of the region's brightest and most massive objects.

[5] As indicated previously, the resemblance of our tracks to traditional ones largely stems from our use of a standard mixing length description of convection.

[6] We are grateful to L. Hillenbrand for supplying these data.

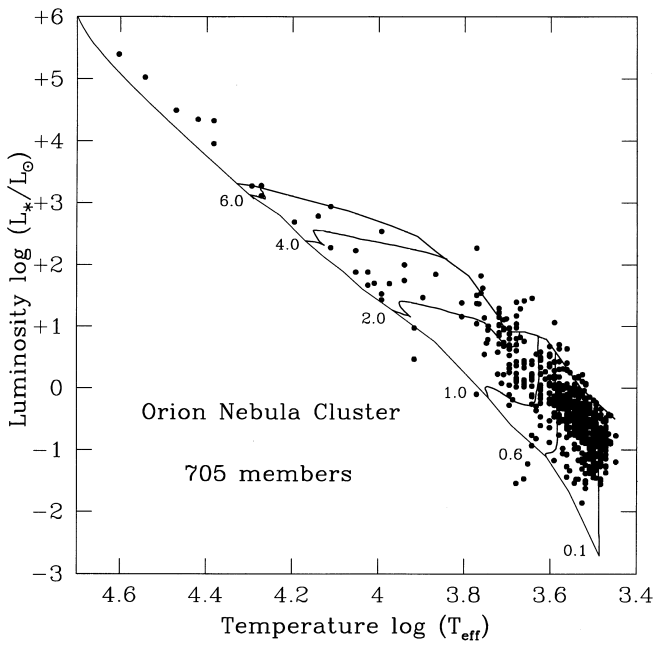


FIG. 3.—H-R diagram for 705 probable members. The birthline, ZAMS, and selected pre–main-sequence tracks are also shown. We have reproduced the ZAMS for $M_* \geq 6\ M_\odot$ from Tout et al. (1996). The luminosity of each star has been corrected to account for the presence of an unresolved companion.

Application of a bolometric correction to an *I*-band flux assumes implicitly that the source in question is a single object. It is by now well established that most pre–main-sequence stars are in fact members of binary systems (Mathieu 1994). Mistaking an unresolved binary for a single star means that the fictitious object has too high a luminosity. Thus, it also has too young an age. Within an entire cluster, the error could materially impact the derived star formation history. In an analysis based on *K*-band surveys, Simon, Ghez, & Leinert (1993) gauged the average age of single stars in Taurus-Auriga to be greater than that of unresolved doubles by a factor of 2–3.

The incidence of binaries in the Orion Nebula Cluster has been investigated by a number of authors. The optical studies of Prosser et al. (1994) and Padgett, Strom, & Ghez (1997) covered the region beyond the innermost 0.1 pc. Here they found a frequency of 13% for visual binaries in the range of 25–800 AU. This figure is consistent with the field-star population, where about 60% of stars have detectable binary companions over all separations (Duquennoy & Mayor 1991; Fischer & Marcy 1992). The Orion figure also accords with lower density star formation regions in the same separation range (see Brandner & Köhler 1998). More recently, Petr et al. (1998) have used a near-infrared speckle holography technique to probe the central region. They estimated a binary fraction of 6% for the low-mass stars with separations between 60 and 225 AU. While again consistent with the field-star result, this fraction is smaller by at least a factor of 2 from that in Taurus-Auriga (e.g., Köhler & Leinert 1998). It is noteworthy that the binary fraction appears to be normal even close to the Trapezium, where the high stellar density might be expected to create frequent disruption. The implication is that the system is too young for many such encounters to have occurred. We shall return to this point later.

Furnished with these observational results, we have treated the binarity issue through an heuristic, statistical approach. We assume for simplicity that every source is an unresolved double, if we were to extend the companions to include as yet undetected brown dwarfs. Specifically, we take the companion masses to be distributed according to a standard field-star initial mass function. We further assume that both the primary and secondary have the same pre–main-sequence age, a supposition that is also bolstered empirically (Hartigan, Strom, & Strom 1994; Brandner & Zinnecker 1997). As detailed in the Appendix, we are then able to derive a correction factor $f$ to the luminosity of any star; this factor depends only on the stellar mass. We have applied this correction to all the 705 stars shown in Figure 3. Note that even under our extreme assumption of complete binarity, the net effect is modest. In particular, we also show in the Appendix that the expected *age* correction, for a primary of solar mass, is about 1.5. This is substantially less than that estimated previously by Simon et al. (1993).

Returning to the H-R diagram of Figure 3, we first note that our calculated birthline indeed delineates the upper envelope to the stellar distribution at low and intermediate masses. This agreement between theory and observation was first noted for T associations (Stahler 1983), and later for a heterogeneous sample of Herbig Ae and Be stars (Palla & Stahler 1990). The present work represents the first such comparison using a single, richly populated cluster that includes both classes of objects.

Our predicted endpoint to the birthline at 8 $M_\odot$ also appears to be supported by the data. That is, more massive stars are grouped tightly about the ZAMS, while less massive ones diverge from it. A very similar pattern is evident in the cluster NGC 6611 (Hillenbrand et al. 1993), in a number of Galactic OB associations (Massey, Johnson, & DeGioia-Eastwood 1995), and in the R136 cluster of 30 Doradus (Massey & Hunter 1998). For the case at hand, we also note an apparent displacement *above* the ZAMS in the data. One cannot invoke post–main-sequence stellar evolution, which would produce too small a shift for any age less than $10^7$ yr (e.g., Schaller et al. 1992). The displacement must therefore reflect systematic errors in the empirical determination of $L_*$, $T_{\rm eff}$, or both. We note in this regard the study of Brown, de Geus, & de Zeeuw (1994), which derived effective temperatures of relatively massive Orion Nebula stars through spectroscopic means. The location of their stars in the H-R diagram is in closer agreement with the ZAMS of Figure 3.

At lower masses, we also find a scattering of stars below the ZAMS and above the birthline. The first effect has long been noted, since the earliest quantitative studies of young clusters (e.g., Walker 1956). Protostar theory can, in principle, accommodate the overly luminous stars through an enhanced accretion rate. However, we are loath to adopt this explanation. Comparison with Figure 12 of Palla & Stahler (1993) indicates that $\dot{M}$ would need to be raised by an order of magnitude, implying rather exotic conditions in dense cores producing low-mass stars. For both types of outliers, a more significant factor is likely to be the difficulty in compensating for anomalous interstellar extinction. A patchy cloud structure is indeed expected within the recently cleared environment of the Orion Nebula.

We now use our tracks and isochrones to determine the masses and ages of the cluster members. Here we exclude all stars ostensibly above the birthline or below the ZAMS,

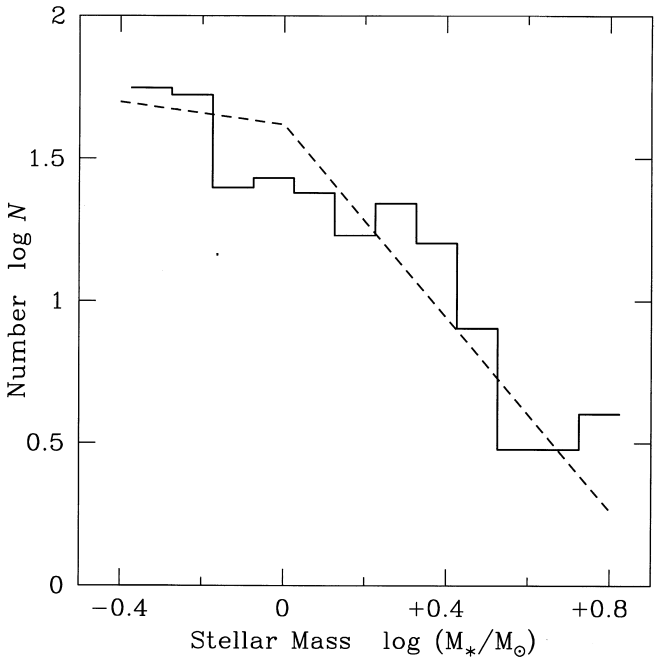


FIG. 4.—Mass distribution of cluster members between 0.4 and 6.0 $M_\odot$. The dashed line represents the field-star initial mass function of Scalo (1998), normalized to the same total number.

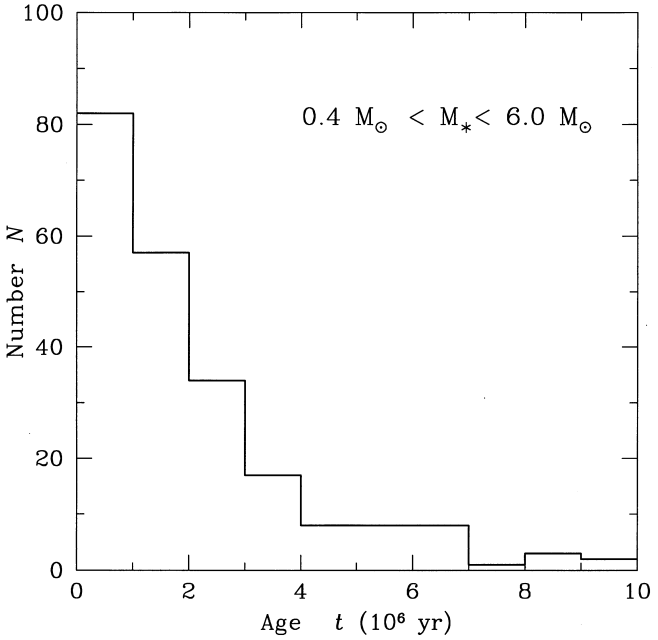


FIG. 5.—Age histogram of the cluster, also in the mass range 0.4–6.0 $M_\odot$.

and (for age determination) those objects more massive than 6.0 $M_\odot$. Our first task is to assess the distribution of stellar masses. To obtain a complete census, we use only those mass bins that are not undercounted because of the inherent flux limit of Hillenbrand's survey. According to her Table 2, the spectroscopic sample is 70% complete for an apparent magnitude $I < 15.5$ mag. Knowing the values of $L_*$, $T_{\rm eff}$, and $A_I$ for each star, we can use the bolometric correction and distance modulus to recover that star's apparent $I$-magnitude. We thus find that all objects with $M_* > 0.4\ M_\odot$ should be unaffected by the flux limit.

Figure 4 displays the mass distribution for stars between 0.4 and 6.0 $M_\odot$. Within this group of 258 stars, the population generally rises toward lower mass, with an apparent plateau between 2.0 and 0.7 $M_\odot$. For $M_* < 0.4\ M_\odot$, a glance at the H-R diagram shows that the number of stars must continue to rise. However, the flux limitation prevents us from gauging this trend quantitatively. The dashed curve in the figure shows the field-star initial mass function recently advocated by Scalo (1998), normalized to our total population. This function is a broken power law of index

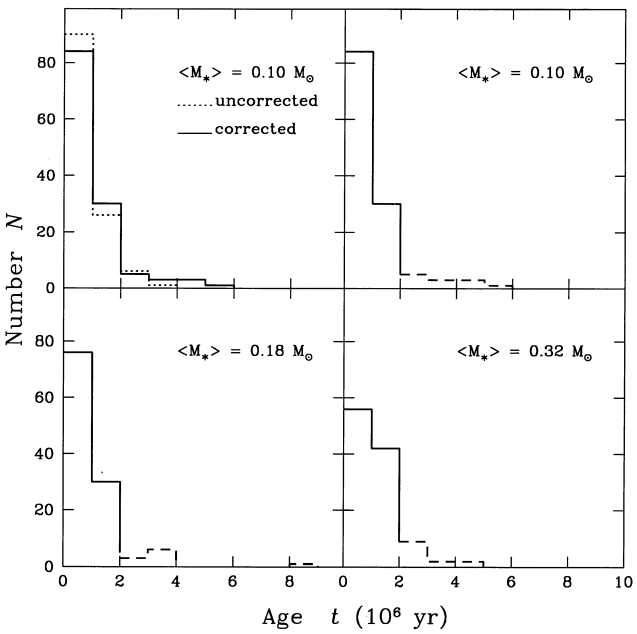


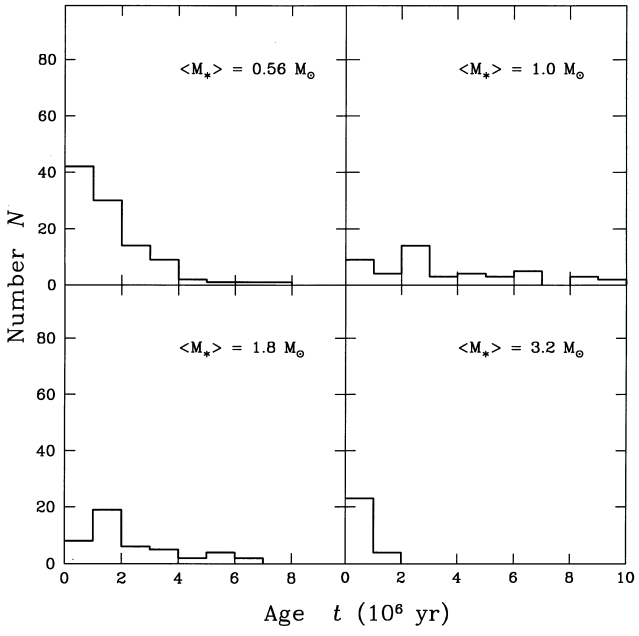


FIG. 6.—*Left*: Mass-specific age histograms (lower masses). The average mass of each group is indicated at the top of its panel. The dashed line indicates bins that are incomplete due to observational sensitivity. The upper left panel shows the change in the age distribution introduced by the luminosity correction for binaries. *Right*: Mass-specific age histograms (higher masses). Note that these groups are not affected by the incompleteness limit.

$-1.7$ in the range 1–10 $M_\odot$, and $-0.2$ at lower masses. It is clear that the field-star result provides a satisfactory, if crude, fit to the data.

Figure 5 is the age histogram of the cluster, employing the same subset from 0.4 to 6.0 $M_\odot$. There was evidently a low level of star formation activity $10^7$ yr in the past, a slow rise, and finally a steep acceleration toward the present epoch. It now becomes clear that our earlier "age" of $2 \times 10^6$ yr represents, in an approximate manner, the total duration of vigorous star formation.

The most striking aspect of Figure 5 is, of course, the sharp rise in stellar births within the recent past. This rise is not restricted to one subset of the population, but occurs globally. To illustrate this fact, Figures 6*a* and 6*b* display histograms for seven mass bins. These bins cover equal logarithmic intervals, and range in central mass from $\log M_\odot = -1.00$ to $\log M_\odot = +0.50$. The lowest masses are subject to the flux limit; we indicate the affected portion of each histogram by a dashed line. Every histogram is further corrected for binaries according to our statistical prescription. The upper left panel shows explicitly for the lowest bin that this correction is minor. We see that the acceleration exhibited by the total population is also present in each subgroup, at least for $M_* \lesssim 1\ M_\odot$. A similar trend is discernible at higher masses, but the numbers soon become too low for statistical significance.

## 5. DISCUSSION

Our analysis of star formation in the Orion Nebula Cluster is based on a single, uniformly constructed set of pre–main-sequence tracks, which both span the requisite mass range and start from physically motivated initial conditions. In contrast, Hillenbrand (1997) interpreted her data through the models of D'Antona & Mazzitelli (1994) from 0.01 to 2.5 $M_\odot$, Swenson et al. (1994) from 3.0 to 5.0 $M_\odot$, and Ezer & Cameron (1965) for all higher masses. These various studies differ markedly in the underlying model assumptions. Such differences, as we stressed in § 2, strongly influence the resulting picture of star formation. One of Hillenbrand's findings, for example, was a systematic increase of stellar age with mass. This correlation would have important implications, but is more plausibly due to an erroneous age assignment at higher masses. In our calculation, where all ages are calibrated by the birthline, no such trend is evident. Hillenbrand also found a sharp turnover in the mass distribution below a few $\times$ 0.1 $M_\odot$. Such a peak would represent a departure from modern results on the general field-star population, where the initial mass function flattens or continues to rise at subsolar values (Kroupa, Tout, & Gilmore 1993; Scalo 1998). As our Figure 4 indicates, this discrepancy also vanishes once we use our tracks to reassess masses and properly account for the flux limitation of the survey. We have also examined the mass distribution for all probable cluster members without regard to the flux limit, and again see no sign of a turnover.

Our studies of both the luminosity function and the H-R diagram concur that star formation has mainly been confined to the last $2 \times 10^6$ yr. The extreme youth of this region is not a new result, of course. The earlier surveys of Herbig & Terndrup (1986) and Prosser et al. (1994) both emphasized this point, as did Brown et al. (1994) in their investigation of the massive population. Indeed, the region is so young that the stars have not had time to move appreciably from their birth sites. Thus, the projected surface density of the visible stars and the contours of $^{13}$CO emission are strikingly similar (L. Hillenbrand & J. Bally 1997, private communication).

Both stars and remnant gas peak sharply at the location of the Trapezium. Now the optically revealed cluster traces the present extent of the spreading H II region. It has long been accepted that both the Trapezium and its H II region lie in front of an opaque portion of the Orion A cloud (Zuckerman 1973). Behind the visible stars, and still partially embedded within the cloud wall, are the additional members thus far detectable only in the near infrared (Ali & Depoy 1995). Still further inside lies the BN-KL region, whose molecular outflows, shocked $H_2$ emission, and maser activity identify it as a site of vigorous ongoing star formation. In summary, the morphology strongly suggests that the Trapezium stars themselves formed in situ, instead of migrating after birth to their present, central location. Bonnell & Davies (1998) have recently quantified this point by demonstrating, through *N*-body simulations, that dynamical mass segregation would require a longer time than any reasonable age estimate for this cluster.

The most novel feature revealed by our age histogram is the pronounced acceleration in star formation activity toward the present epoch. In fact, however, a similar trend has already been noted in other regions. Palla & Galli (1997) found a rising star formation rate in Taurus, Lupus, and Chamaeleon, albeit at a reduced level. Martín et al. (1998) analyze the optically visible stars of $\rho$ Ophiuchi and also note a recent increase in activity. Finally, Luhman et al. (1998) have placed about 100 members of IC 348 in the H-R diagram. We have reanalyzed their data using our tracks, and again find a peak in star formation within the last $2 \times 10^6$ yr, and very few members older than $5 \times 10^6$ yr.

It thus appears that star formation may proceed in an accelerated manner within a wide range of environments. If confirmed by future studies, such a trend would be an important clue in the puzzle of how clusters originate from their parent clouds. These latter entities are either the clumps of giant complexes (in the case of OB associations such as those of Orion), or the more isolated dark clouds that produce T associations. It is believed that all such structures are primarily supported against self-gravity through the effective pressure from magnetohydrodynamic (MHD) waves (McKee et al. 1993). Gradual dissipation of these waves should result in overall cloud contraction (McKee 1989; Elmegreen & Combes 1992). Suppose now that the local star formation rate increases with cloud density, at least above some threshold value. Then the observed acceleration may reflect a similar trend in the rate of cloud contraction.

Returning to the Orion Nebula Cluster, the gas dispersal from the Trapezium implies that the present-day stellar production rate in the vicinity is very low. Thus, the formation history portrayed in Figure 5 should more correctly include a steep plunge near $t = 0$. This decline must occur over an interval shorter than the effective temporal resolution of the histogram, or about $10^6$ yr. Both the formation of the O stars and their clearing of gas out to the present cluster boundary must have occurred within this relatively brief period. As noted before, star formation continues in the highly embedded BN-KL region, which is behind the ionization front. We note finally that a recent origin for the Trapezium itself is also indicated by the presence of illuminated disks (proplyds) around nearby low-mass stars

(O'Dell 1998). According to current theory, the ultraviolet flux from $\theta^1$ C alone is sufficient to ablate such structures within a time of the order of $10^5$ yr (Johnstone, Hollenbach, & Bally 1998).

The parent cloud giving rise to the Orion Nebula Cluster must have begun its contraction some $10^7$ yr ago. This process gradually accelerated until, within the last $2 \times 10^6$ yr, the density climbed high enough to form copious stars, with a mass distribution similar to the field. Note that our Figure 3 indicates substantial production within the brown dwarf regime. In any case, it is important to bear in mind that the cluster in this earliest phase was *not* a pure $N$-body system, but consisted of protostars and pre–main-sequence stars embedded in a dense background gas. In at least one location, the combined stellar and gas density rose to a very high peak. It was here that the massive stars of the Trapezium formed quickly and dispersed a portion of the larger cloud complex.

There is a growing body of evidence that high-mass stars are *always* born in crowded environments. Indeed, their formation mechanism may be qualitatively different from that pictured in current protostar theory, and may entail the coalescence of lower mass objects (Bonnell, Bate, & Zinnecker 1998; Stahler, Palla, & Ho 1999). Both the proximity of the Orion Nebula Cluster and its extraordinary density are favorable for empirical study of this issue. We mentioned, for example, that the binary fraction appears to be similar to that in the field-star population. Future observational studies might focus on the detailed variation of stellar multiplicity as a function of distance from the Trapezium. A clear increase toward the crowded center, particularly among stars of intermediate and higher mass, would bolster the idea of coalescence. One indication of this trend comes from Petr et al. (1998), who indeed find a higher binary fraction among the more massive Orion stars, although at a low statistical significance. Mason et al. (1998) have examined a large sample of O stars in Galactic clusters and associations. They also note a relatively high proportion of single-line spectroscopic binaries.

We close by remarking that the very notion of globally accelerating star formation is difficult to reconcile with the current theory of dense cores. It is generally believed that an individual core contracts through ambipolar diffusion before undergoing gravitational collapse at its center. The most detailed calculations to date find that the contraction lasts about $10^7$ yr (Basu & Mouschovias 1995). On the other hand, we have just seen that the H-R diagram of at least one cluster shows a much more rapid onset for star formation activity. More to the point, there is no indication from the theoretical studies that neighboring cores should appreciably influence one another in forming stars. A more plausible interpretation of the data is that many cores are evolving nearly synchronously, in response to a common, external stimulus. It is time for both observers and theorists to begin addressing this issue, by probing the physical link between a dense core and its changing background medium.

We thank Ian Bonnell, Lynne Hillenbrand, Mark McCaughrean, and Hans Zinnecker for illuminating discussions on various aspects of this problem. Part of our research has been supported by ASI grant ARS 96-66 to the Osservatorio di Arcetri. Funding for S. W. S. was provided by the NASA Astrophysics Theory Program grant NAGW-3107.

## APPENDIX A

## STATISTICAL CORRECTION FOR UNRESOLVED BINARIES

Suppose a pre–main-sequence star is observed to have luminosity $L_*$ and effective temperature $T_{\rm eff}$. Suppose also that this object is known to be on the convective (vertical) portion of its evolutionary track. From the temperature and luminosity, we can estimate the star's age. For present purposes, we can take this age to be the Kelvin-Helmoltz contraction time,

$$t \equiv \frac{GM_*^2}{R_* L_*}, \tag{A1}$$

where $M_*$ and $R_*$ are the stellar mass and radius.

For convective solar-type pre–main-sequence stars, the effective temperature is related to the mass by the approximate relation

$$T_{\rm eff} = \bar{T}\left(\frac{M_*}{\bar{M}}\right)^n, \tag{A2}$$

where $n \sim 0.2$, and where $\bar{M}$ and $\bar{T}$ are a fiducial mass and temperature, respectively. In addition, we can use the blackbody law to relate $R_*$ to $T_{\rm eff}$ and $L_*$. We find

$$t = \frac{G\bar{M}(T_{\rm eff}/\bar{T})^{2/n}(4\pi\sigma T_{\rm eff}^4)^{1/2}}{L_*^{3/2}}, \tag{A3}$$

where $\sigma$ is the Boltzmann constant.

It turns out that the "star" is not a single object, but an unresolved binary. Let $q$ be the ratio of the mass of the unseen companion, $M_2$, to the mass of the primary star, $M_1$. What is the actual luminosity of the two stars as a function of $q$? In addition, given a reasonable distribution of secondary masses, what is the *average* luminosity ratio?

To answer the first question, we assume that the two stars have precisely the same age. If $T_2$ is the temperature of the unseen companion, then, since the two luminosities, $L_1$ and $L_2$, together give $L_*$, the equal-age requirement becomes, by equation (A3),

$$\frac{(T_1/\bar{T})^{2/n}T_1^2}{L_1^{3/2}} = \frac{(T_2/\bar{T})^{2/n}T_2^2}{(L_* - L_1)^{3/2}} . \tag{A4}$$

Using equation (A2) to evaluate the temperatures, we find a simple expression for $L_1$:

$$\frac{L_1}{L_*} = [1 + q^{4(1+n)/3}]^{-1} \tag{A5}$$

$$\equiv f(q) \tag{A6}$$

In order to compute the reduction factor $f(q)$, we must specify the distribution of secondary masses. Here we adopt the initial mass function for field stars, an assumption that apparently holds for at least G- and M-type primaries (Duquennoy & Mayor 1991; Fischer & Marcy 1992). We utilize the result of Kroupa, Tout, & Gilmore (1993), which includes a slope change at subsolar mass:

$$\xi(M_*) = \begin{cases} K(M_*/0.08\ M_\odot)^{-1.3}, & 0.08 < M_*/M_\odot < 0.5\ ; \\ 0.092K(M_*/0.5\ M_\odot)^{-2.2}, & 0.5 < M_*/M_\odot < 1.0; \\ 0.020K(M_*/1.0\ M_\odot)^{-2.7}, & 1.0 < M_*/M_\odot\ , \end{cases} \tag{A7}$$

where $K = 4.41$ is the normalization constant obtained by requiring that $\int_0^\infty \xi(M_*)\, dM_* = 1$. For masses below the minimum value of 0.08 $M_\odot$, we have assumed that the mass function is constant and equal to $K$. The average value of $f(q)$, which we denote simply as $f$, is then

$$f \equiv \int_0^1 f(q)\, \xi(q)\, dq\ , \tag{A8}$$

where

$$\xi(q) \equiv \xi(qM_1/M_\odot)M_1/M_\odot\ , \tag{A9}$$

so that $\int_0^\infty \xi(q)\, dq = 1$. Note that $f$ depends on the primary mass $M_1$ and can readily be evaluated numerically from equation (A7). Figure 7 shows the variation of the luminosity reduction factor as a function of $M_1$. The factor is only small for the

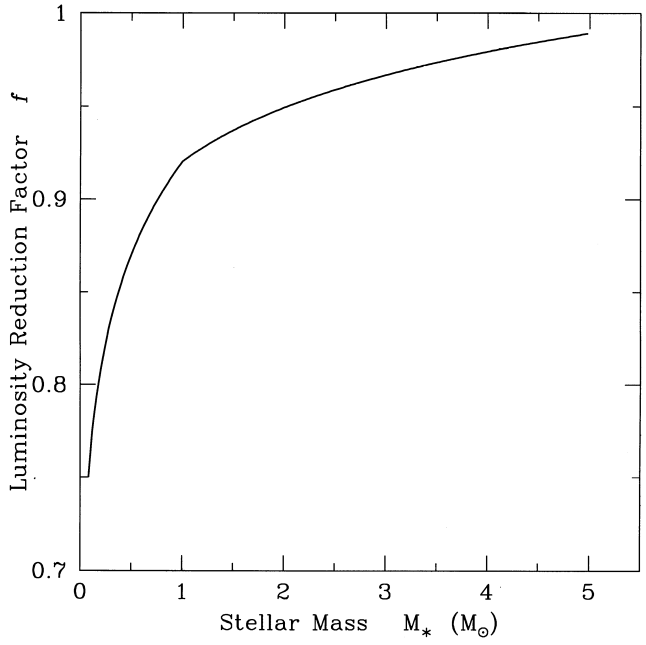


FIG. 7.—Luminosity reduction factor as a function of stellar mass

lowest mass values, and rises to 0.75 by $M_1 = 0.08\ M_\odot$. Thus, the primary luminosity could be overestimated by at most 25%. The dashed line in Figure 7 is an analytic fit given by

$$f = \begin{cases} 0.75(M_1/0.08)^{0.081}\ , & 0.08 \le M_1/M_\odot \le 1.0\ ; \\ 0.93(M_1/1.0)^{0.045}\ , & 1.0 < M_1/M_\odot \le 5.0\ ; \\ 1.0\ , & 5.0 < M_1/M_\odot\ . \end{cases} \tag{A10}$$

We can also estimate the error in age introduced by an unseen companion. From equation (A3), we first obtain $t_1(q)$, the true primary age as a function of $q$:

$$t_1(q) = \frac{G\bar{M}(T_{\rm eff}/\bar{T})^{2/n}(4\pi\sigma T_{\rm eff}^4)^{1/2}}{[f(q)]^{3/2}L_*^{3/2}}\ . \tag{A11}$$

Here we have assumed that $T_1 = T_{\rm eff}$, i.e., that the observed surface temperature corresponds to that of the primary. The ratio of the true age to the naïve value $t_0$ from equation (A1) is then

$$\frac{t_1(q)}{t_0} = [f(q)]^{-3/2}\ . \tag{A12}$$

The *maximum* age discrepancy corresponds to $q = 1$. Evaluating $f(1)$ from equation (A5), we find that the corresponding ratio $t_1/t_0$ is 2.83. An age ratio of 2.0 requires a $q$-value of 0.7.

In fact, such relatively high companion masses are unlikely. Once again, the average age discrepancy is obtained by folding in the expected distribution of mass ratios, $\xi(q)$. We now specialize to the case of a primary mass near 1 $M_\odot$. According to Duquennoy & Mayor (1991), the appropriate $q$-distribution is approximately Gaussian,

$$\xi(q) = H\ \exp\left[-\frac{(q-\mu)^2}{2\sigma^2}\right], \tag{A13}$$

where $\mu = 0.23$, $\sigma = 0.42$, and $H$ is the normalization constant. This 1 $M_\odot$ result agrees with our more general one from equation (A7). The mean value of $q$, according to equation (A10), is only 0.23. The average age ratio is

$$\left\langle \frac{t_1}{t_0} \right\rangle = \int_0^1 [f(q)]^{-3/2}\xi(q)\,dq\ . \tag{A14}$$

Evaluating the integral numerically, we find this ratio to be 1.46.

## REFERENCES


Alexander, D. R., & Ferguson, J. W. 1994, ApJ, 437, 879
Alexander, D. R., Johnson, H. R., & Rypma, R. L. 1983, ApJ, 272, 773
Alexander, D. R., Tamanai, A., Allard, F., & Ferguson, J. W. 1998, BAAS, 192, 6716
Ali, B., & Depoy, D. L. 1995, AJ, 109, 709
Allard, F., Hauschildt, P. H., Alexander, D. R., & Starrfield, S. 1997, ARA&A, 35, 137
Basu, S., & Mouschovias, T. Ch. 1995, ApJ, 453, 271
Beckwith, S. V. W., Sargent, A. I., Chini, R. S., & Güsten, R. 1990, AJ, 99, 924
Bessell, M. S. 1998, in IAU Symp. 189, Fundamental Stellar Properties: The Interaction between Observation and Theory, ed. T. R. Bedding, A. J. Booth, & J. Davis (Dordrecht: Reidel), 127
Bodenheimer, P. 1966, ApJ, 144, 709
Bonnell, I., Bate, M. R., & Zinnecker, H. 1998, MNRAS, 298, 93
Bonnell, I., & Davies, M. B. 1998, MNRAS, 295, 691
Bouvier, J., & Appenzeller, I. 1992, A&AS, 92, 481
Brandner, W., & Köhler, R. 1998, ApJ, 499, L79
Brandner, W., & Zinnecker, H. 1997, A&A, 321, 220
Brown, A. G. A., de Geus, E. J., & de Zeeuw, P. T. 1994, A&A, 289, 101
Calvet, N., Patino, A., Magris, G. C., & D'Alessio, P. 1991, ApJ, 380, 617
Canuto, V. M., & Mazzitelli, I. 1991, ApJ, 370, 295
Chabrier, G., & Baraffe, I. 1997, A&A, 327, 1039
Clayton, D. D. 1983, Principles of Stellar Evolution and Nucleosynthesis (New York: Gordon & Breach), chap. 5
D'Antona, F., & Mazzitelli, I. 1994, ApJS, 90, 467
———. 1998, in Cool Stars in Clusters and Associations, ed. G. Micela, R. Pallavicini, & S. Sciortino, Mem. Soc. Astron. Italiana, 68, 807
Duquennoy, A., & Mayor, M. 1991, A&A, 248, 485
Edwards, S., Ray, T., & Mundt, R. 1993, in Protostars and Planets III, ed. E. H. Levy & J. I. Lunine (Tucson: Univ. Arizona Press), 567
Eggleton, P., Faulkner, J., & Flannery, B. P. 1973, A&A, 23, 325
Elmegreen, B. G., & Combes, F. 1992, A&A, 259, 232
Ezer, D., & Cameron, A. G. W. 1965, Canadian J. Phys., 14, 1497
Fischer, D. A., & Marcy, G. W. 1992, ApJ, 396, 178
Fletcher, A. B., & Stahler, S. W. 1994a, ApJ, 435, 313
———. 1994b, ApJ, 435, 329
Forestini, M. 1994, A&A, 285, 473
Foster, P. N., & Chevalier, R. A. 1993, ApJ, 416, 303
Geiss, J., & Gloeckler, G. 1998, Space Sci. Rev., 84, 275
Grossman, A. S., & Graboske, H. C. 1973, ApJ, 180, 195
Gullbring, E., Hartmann, L., Briceño, C., & Calvet, N. 1998, ApJ, 492, 323
Hartigan, P., Edwards, S., & Ghandour, L. 1995, ApJ, 452, 736
Hartigan, P., Strom, K. M., & Strom, S. E. 1994, ApJ, 427, 961
Hartmann, L., Calvet, N., Gullbring, E., & D'Alessio, P. 1998, ApJ, 495, 385
Hayashi, C. 1961, PASJ, 13, 450
Herbig, G. H., & Terndrup, D. M. 1986, ApJ, 307, 609
Hillenbrand, L. A. 1997, AJ, 113, 1733
Hillenbrand, L .A., Massey, P., Strom, S. E., & Merrill, K. M. 1993, AJ, 106, 1906
Hillenbrand, L. A., Strom, S. E., Calvet, N., Merrill, K. M., Gatley, I., Makidon, R. B., Meyer, M. R., & Skrutskie, M. F. 1998, AJ, 116, 1816
Hirth, G. A., Mundt, R., & Solf, J. 1997, A&AS, 126, 437
Iben, I. 1965, ApJ, 141, 993
Iglesias, C. A., & Rogers, F. J. 1991, ApJ, 371, L73
———. 1996, ApJ, 464, 943
Johnstone, D., Hollenbach, D., & Bally, J. 1998, ApJ, 499, 758
Kenyon, S. J., & Hartmann, L. 1995, ApJS, 101, 117
Kirkpatrick, J. D., Kelly, D. M., Rieke, G. H., Liebert, J., Allard, F., & Wehrse, R. 1993, ApJ, 402, 643
Köhler, R., & Leinert, Ch. 1998, A&A, 331, 997
Kroupa, P., Tout, C. A., & Gilmore, G. 1993, MNRAS, 262, 545
Lada, E. A., & Lada, C. J. 1995, AJ, 109, 1682
Larson, R. B. 1972, MNRAS, 157, 121
Leggett, S. K., Allard, F., Berriman, G., Dahn, C. C., & Hauschildt, P. H. 1996, ApJS, 104, 117
Li, Z.-Y. 1998, ApJ, 497, 850
Linsky, J. L. 1998, Space Sci. Rev., 84, 285
Luhman, K. L., Rieke, G. H., Lada, C. J., & Lada, E. A. 1998, ApJ, 508, 347
Martín, E. L., Montmerle, T., Gregorio-Hetem, J., & Casanova, S. 1998, MNRAS, 300, 733
Mason, B. D., Gies, D. R., Hartkopf, W. I., Bagnuolo, W. G., Jr., ten Brummelaar, T., & McAlister, H. A. 1998, AJ, 115, 821
Massey, P., & Hunter, D. A. 1998, ApJ, 493, 180
Massey, P., Johnson, K. E., & DeGioia-Eastwood, K. 1995, ApJ, 454, 151
Masunaga, H., Miyama, S. M., & Inutsuka, S.-I. 1998, ApJ, 495, 346
Mathieu, R. D. 1994, ARA&A, 32, 465

McCaughrean, M. J., & Stauffer, J. R. 1994, AJ, 108, 1382
McKee, C. F. 1989, ApJ, 345, 782
McKee, C. F., Zweibel, E. G., Goodman, A. A., & Heiles, C. 1993, in Protostars and Planets III, ed. E. H. Levy & J. I. Lunine (Tucson: Univ. Arizona Press), 327
Meynet, G., Mermilliod, J.-C., & Maeder, A. 1993, A&AS, 98, 477
Mihalas, D., Däppen, W., & Hummer, D. G. 1988, ApJ, 331, 815
O'Dell, C. R. 1998, AJ, 115, 263
Padgett, D. L., Strom, S. E., & Ghez, A. M. 1997, ApJ, 477, 705
Palla, F., & Galli, D. 1997, ApJ, 476, L35
Palla, F., & Stahler, S.W. 1990, ApJ, 360, L47
———. 1991, ApJ, 375, 288
———. 1992, ApJ, 392, 667
———. 1993, ApJ, 418, 414
Petr, M., Coudé du Foresto, V., Beckwith, S. V. W., Richichi, A., & McCaughrean, M. J. 1998, ApJ, 500, 825
Pinsonneault, M. H., Stauffer, J., Soderblom, D. R., Jones, B. F., & Hanson, R. B. 1998, ApJ, 504, 170
Pols, O. R., Tout, C. A., Eggleton, P. P., & Han, Z. 1995, MNRAS, 274, 964
Prosser, C. F., Stauffer, J. R., Hartmann, L., Soderblom, D. R., Jones, B. F., Werner, M. W., & McCaughrean, M. J. 1994, ApJ, 421, 517
Prusti, T. 1999, in The Universe as Seen by ISO, ed. P. Cox & M. Kessler (ESA SP-427; Garching: ESA), in press
Rogers, F. J., Swenson, F. J., & Iglesias, C. A. 1996, ApJ, 456, 902
Safier, P., McKee, C. F., & Stahler, S. W. 1997, ApJ, 485, 660
Saumon, D., Chabrier, G., & Van Horn, H. M. 1995, ApJS, 99, 713
Scalo, J. M. 1998, in ASP Conf. Ser. 142, The Stellar Initial Mass Function, ed. G. Gilmore & D. Howell (San Francisco: ASP), 201
Schaller, G., Schaerer, D., Meynet, G., & Maeder, A. 1992, A&AS, 96, 269
Simon, M., Ghez, A. M., & Leinert, Ch. 1993, ApJ, 408, L33
Stahler, S. W. 1983, ApJ, 274, 822
———. 1988, ApJ, 332, 804
———. 1989, ApJ, 347, 950
Stahler, S. W., Palla, F., & Ho, P. T. P. 1999, in Protostars and Planets IV, ed. V. Mannings, A. P. Boss, & S. S. Russell (Tucson: Univ. Arizona Press), in press
Stahler, S. W., Shu, F. H., & Taam, R. E. 1980, ApJ, 241, 637
Swenson, F. J., Faulkner, J., Rogers, F. J., & Iglesias, C. A. 1994, ApJ, 425, 286
Tout, C. A., Pols, O. R., Eggleton, P. P., & Han, Z. 1996, MNRAS, 281, 257
Ventura, P., Zeppieri, A., Mazzitelli, I., & D'Antona, F. 1998, A&A, 331, 1011
Vidal-Majar, A., Ferlet, R., & Lemoine, M. 1998, Space Sci. Rev., 84, 297
Viti, S., Jones, H. R. A., Schweitzer, A., Allard, F., Hauschildt, P. H., Tennyson, J., Miller, S., & Longmore, A. J. 1997, MNRAS, 291, 780
Walker, M. F. 1956, ApJS, 2, 365
Wilking, B. A., Lada, C. J., & Young, E. T. 1989, ApJ, 340, 823
Zinnecker, H., McCaughrean, M. J., & Wilking, B. A. 1993, in Protostars and Planets III, ed. E. H. Levy & J. I. Lunine (Tucson: Univ. Arizona Press), 429
Zuckerman, B. 1973, ApJ, 183, 863